Computing Activity Coefficients of Binary Lennard-Jones Mixtures by Gibbs-Duhem Integration

By Dietmar Paschek[1,*], Alfons Geiger[1], Jan Fischer[2], and Gabriele Sadowski[2]

[1] Physikalische Chemie, Otto-Hahn-Str. 6, TU Dortmund, D-44221 Dortmund, Germany
[2] Lehrstuhl für Thermodynamik, Emil-Figge-Str. 70, TU Dortmund, D-44227 Dortmund, Germany

We determine activity coefficients of both components of different binary Lennard-Jones mixtures obtained at $T^* = 2.0$ and $\rho^* = 0.6$ by using two different strategies: (i) direct evaluation of the excess chemical potentials of both components applying the potential distribution theorem, and (ii) using the Gibbs-Duhem integration based on the activity coefficients of the counter-component, which was calculated directly from the potential distribution theorem approach. Both methods lead numerically to similar results and therefore offer a route to determine activity coefficients of mixtures with large complex molecules by alternatively calculating chemical potentials of potentially simpler counter-constituents.

1. Introduction

The Gibbs-Duhem integration technique represents a rather familiar approach to determine activity coefficients of individual components in liquid mixtures [1]. The calculation is typically based on the measurement of partial pressures of one or several components of the liquid mixture, exploiting the fact that activities are related with respect to one another by the Gibbs-Duhem relation. Hence, also activity coefficients of components might be determined, which exhibit an almost vanishing partial pressure, thus preventing any direct activity determination. Here we show that the Gibbs-Duhem integration strategy might be also applied to directly estimate activity coefficients from computer simulations of complex

---

* Corresponding author. E-mail: dietmar.paschek@udo.edu

fluid mixtures. In perspective, activity coefficients of components might be calculated, which could not be evaluated directly otherwise, such as for large molecules like polymers or proteins. For demonstration purposes we perform simulations for a rather simplified example of fluid mixtures: a binary Lennard-Jones mixture. Applying the potential distribution theorem [2, 3], we calculate the excess chemical potential of both components for different compositions covering a certain part of the composition range, and thus determine the activity coefficients. In a second step we show that a similar result might be obtained by Gibbs-Duhem integration of the chemical potential of the corresponding counter-components.

2. Methods

2.1 Outline of the MD simulations

We perform molecular dynamics (MD) simulations of binary Lennard-Jones (LJ) mixtures consisting of 512 LJ-particles with varying composition. The simulations were performed under constant pressure and constant temperature conditions using a Verlet integrator [4]. A reduced timestep of $\delta t^* = 0.005$ was applied in all cases. The Lennard-Jones interactions were truncated at a cutoff distance of $R_{cut} > 4\sigma$. An initial equilibration run of 10^4 timesteps was followed by a production run of 5×10^5 timesteps, which was used for analysis. Long-range corrections for energy and pressure were applied. We employ the GROMACS simulation program for all MD simulations [5]. The temperatures were fixed at $T^* = 2.0$ by using the Nosé–Hoover thermostat [6, 7] with a reduced coupling time of $\tau^* = 0.5$, and the Parrinello-Rahman barostat with a reduced coupling time of $\tau^* = 1.0$. Fixing the system at a reduced pressure of $P^* = 1.755$ is leading to a reduced equilibrium density of $\rho^* = 0.599$ for the pure LJ-liquid (component B), matching exactly the data reported by Johnson et al. [8]. Here we show simulation results of two types of binary LJ mixtures with parameters of $\sigma_{AA} = \sigma_{BB}$, and varying interaction strengths of $\varepsilon_{AA} = 1.33 \times \varepsilon_{BB}$, and $\varepsilon_{AA} = 2.00 \times \varepsilon_{BB}$. The A-B cross interactions were obtained applying standard Lorentz-Berthelot mixing rules with $\varepsilon_{AB} = (\varepsilon_{AA}\varepsilon_{BB})^{1/2}$. The simulations cover the entire composition range of both mixtures.

2.2 Activity coefficients from the potential distribution theorem

The chemical potential of a single component α in a fluid mixture is given according to

$$\beta\mu_\alpha = \beta\mu_\alpha^\circ + \ln a_\alpha, \tag{1}$$

where $\beta = 1/k_B T$, a_α is the activity, and μ_α° represents the chemical potential at the reference state. The activity is expressed as $a_\alpha = \gamma_\alpha x_\alpha$, where x_α is the mole

fraction of component α, and γ_α is the corresponding activity coefficient. According to the potential distribution theorem [2, 3] (also known as Widom particle insertion technique), the chemical potential of the monoatomic component α can be expressed as

$$\beta\mu_\alpha = \ln\frac{\Delta(N_\alpha,\ldots,P,\beta)}{\Delta(N_\alpha+1,\ldots,P,\beta)}$$

$$= \ln\frac{(N_\alpha+1)\Lambda_\alpha^3}{<V>} + \ln\frac{<V>}{<Ve^{-\beta\Delta U_\alpha}>}, \tag{2}$$

where $\Delta(\ldots)$ is the isobar isothermal partition function, and $<\ldots>$ denotes isobar-isothermal averaging. Λ_α is the thermal wavelength of particle α, V is the Volume and N_α is the number of particles α. ΔU_α is the energy of a virtual particle of type α, randomly inserted to the system [2], leading to the excess chemical potential contribution with respect to the ideal gas state of

$$-\beta\mu_{\alpha,\text{ex}} = \ln\left[<V\exp(-\beta\Delta U_\alpha)> / <V>\right]. \tag{3}$$

Subtracting the chemical potential at the reference state "°", and recognizing that $x_\alpha = N_\alpha/N$, we obtain

$$\beta\mu_\alpha - \beta\mu_\alpha^\circ = \ln a_\alpha$$

$$= \ln\left[\frac{(Nx_\alpha+1)<Ve^{-\beta\Delta U_\alpha}>_{x_\alpha=x^\circ}}{(Nx^\circ+1)<Ve^{-\beta\Delta U_\alpha}>_{x_\alpha}}\right]. \tag{4}$$

a_α might be also expressed in terms of the corresponding calculated excess chemical potentials

$$a_\alpha = \frac{(Nx_\alpha+1)\rho e^{-\beta\mu_{\alpha,\text{ex}}^\circ}}{(Nx^\circ+1)\rho^\circ e^{-\beta\mu_{\alpha,\text{ex}}}}. \tag{5}$$

As reference state "°", we might either consider the pure liquid ($x_\alpha = x^\circ = 1$), or the state of infinite dilution ($x_\alpha = x^\circ = 0$). Hence, the activity coefficient γ_α of component α in the mixture with composition x_α is given by

$$\gamma_\alpha = \frac{(N+x_\alpha^{-1})\rho e^{-\beta\mu_{\alpha,\text{ex}}^\circ}}{(Nx^\circ+1)\rho^\circ e^{-\beta\mu_{\alpha,\text{ex}}}}. \tag{6}$$

Please note that $\gamma_\alpha \to 1$ upon approaching the reference state with $x_\alpha \to x^\circ$, and that $\gamma_\alpha > 1$ indicates either weakening of intermolecular interactions and/or a decrease in volume.

The Boltzmann terms in Eq. 6 were calculated by random Monte Carlo insertions of particles of type *A* and *B* into the configurations obtained from the MD simulations. In order to perform the numerical evaluation of the excess chemical potential contributions efficiently, we have used an excluded volume map (EVM) [9], projecting the occupied volume onto a grid of approximately $0.13 \times \sigma$
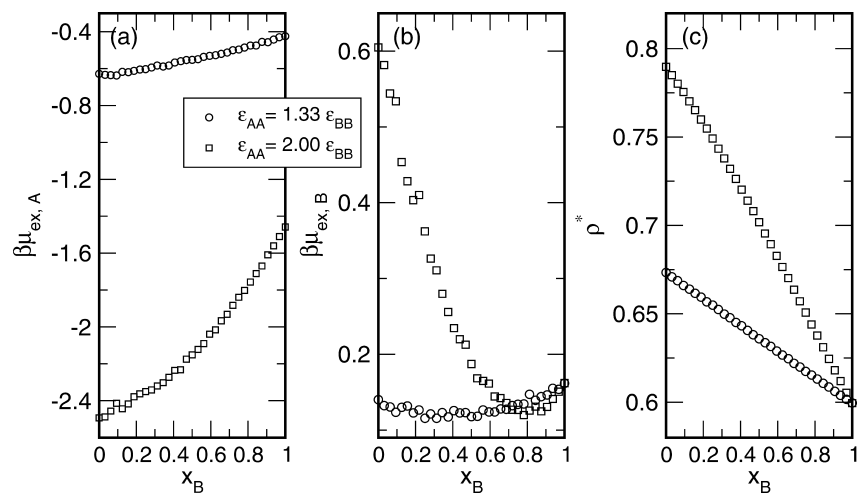
Fig. 1. Excess chemical potentials μ_{ex} of the components *A* (a) and *B* (b), as well as the corresponding densities $\rho^* = N\sigma_{BB}^3/V$ (c) for the LJ-mixtures with $\varepsilon_{AA}/\varepsilon_{BB} = 1.33$, and $\varepsilon_{AA}/\varepsilon_{BB} = 2.0$, simulated at $T^* = 2.0$ and $P^* = 1.755$.
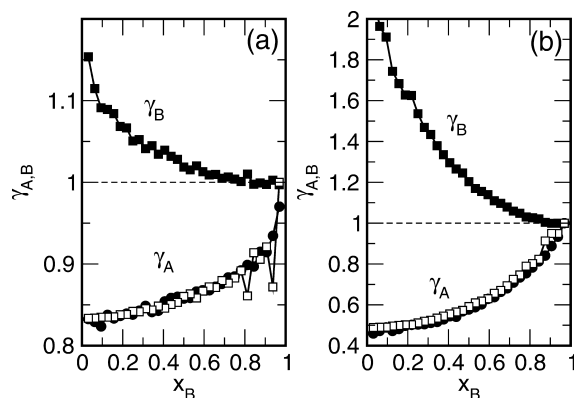

Fig. 2. Comparison of the computed activity coefficients for the two different types of mixtures (a) $\varepsilon_{AA} = 1.33\,\varepsilon_{BB}$ and (b) $\varepsilon_{AA} = 2.0\,\varepsilon_{BB}$. Solid Symbols: Activity coefficients γ_A and γ_B, calculated directly from the excess chemical potentials of components *A* and *B* in the mixture. Open Symbols: Activity coefficients γ_A, computed from γ_B, by numerically integrating the Gibbs-Duhem relation.

mesh-width. Distances smaller than $0.7 \times \sigma$ with respect to any LJ-molecule were neglected and the corresponding term $\exp(-\beta\Delta U_\alpha)$ taken to be zero. About 1000 *successful* (nonzero) particle insertions were sampled for each configuration and 2500 configurations were analyzed for each composition.

2.3 Gibbs-Duhem integration

Starting from the Gibbs-Duhem relation for a binary system

$$0 = N_A \, d\mu_A + N_B \, d\mu_B, \tag{7}$$

we arrive at

$$x_A \, d \ln a_A = -x_B \, d \ln a_B, \tag{8}$$

by inserting $x_\alpha = N_\alpha / N$ and expressing the chemical potentials by their corresponding activities. Hence, the activity of component A can be calculated by integrating activities obtained from component B following

$$\int d \ln a_A = - \int \frac{x_B}{1 - x_B} \, d \ln a_B. \tag{9}$$

In order to avoid the diverging behavior at $x_A \to 1$, the calculation is started at finite concentrations of A, making use of approaching Henry's law, leading to $a_A \to x_A$ and thus $\gamma_A \to 1$. We will consider component (A) as "solute" and component (B) as "solvent". Consequently, we are taking the pure liquid state of component (B) as a reference state for both components. Since the data is available as discretized information at fixed compositions $x_{\alpha,i}$, we have to perform the integration numerically, applying the recursion formula

$$\ln a_{A,i+1} = \ln a_{A,i} +$$
$$\frac{(\ln a_{B,i+1} - \ln a_{B,i})(x_{B,i} + x_{B,i+1})}{x_{B,i} + x_{B,i+1} - 2}. \tag{10}$$

Recognizing the $a_A \to x_A$, for $x_A \to 0$, we are starting the recursion at $\ln a_{A,1} = \ln x_{A,1}$, assuming $\gamma_{A,1} = 1$.

3. Discussion

Table 1 and 2 contain the excess chemical potentials, calculated for the entire composition range of the two different types of mixtures. The error is estimated to be about ± 0.003 in units of β^{-1}. A moderately increasing interaction strength of particles of type A, as shown for the case of $\varepsilon_{AA} = 1.33 \times \varepsilon_{BB}$ in Fig. 1a and 1b, leads to a lowering of the excess chemical potential for both components. In parallel, the density is found to increase, with increasing amount of A, as shown in Fig. 1c. Please note that chemical potential of component B passes through a shallow minimum at $x_B \approx 0.3$, indicating that the decreasing amount of free volume in the dense solution with $x_B \to 0$ creates an increasingly less favourable environment for component B. Here, the volume effect is apparently compensating, and finally even overcompensating the strengthened attractive interactions. This behavior is found to be strongly amplified, upon a further increase of interaction strength of particles A for the mixtures with $\varepsilon_{AA} = 2.0 \times \varepsilon_{BB}$. Again, the chemical potential of component A is found to decrease monotonously. However,

Table 1. Excess chemical potentials $\mu_{ex,\alpha}$ and activities a_α obtained for the Lennard-Jones mixtures with $\sigma_{AA} = \sigma_{BB}$, and $\varepsilon_{AA} = 1.33 \times \varepsilon_{BB}$, simulated at $T^* = 2.0$ and $P^* = 1.755$. The shown density values are according to $\rho^* = N\sigma_{BB}/V$. The data were obtained from the potential distribution theorem [2, 3].

ρ^*	x_B	$\beta\mu_{A,ex}$	$\beta\mu_{B,ex}$
0.6733	0.00000	−0.628	0.140
0.6709	0.03125	−0.634	0.132
0.6687	0.06250	−0.635	0.131
0.6661	0.09375	−0.638	0.123
0.6639	0.12500	−0.618	0.130
0.6616	0.15625	−0.619	0.132
0.6594	0.18750	−0.612	0.123
0.6567	0.21875	−0.605	0.126
0.6548	0.25000	−0.604	0.115
0.6525	0.28125	−0.595	0.121
0.6499	0.31250	−0.584	0.115
0.6477	0.34375	−0.589	0.123
0.6451	0.37500	−0.584	0.117
0.6432	0.40625	−0.568	0.126
0.6406	0.43750	−0.559	0.123
0.6382	0.46875	−0.553	0.123
0.6358	0.50000	−0.552	0.118
0.6336	0.53125	−0.548	0.118
0.6315	0.56250	−0.536	0.127
0.6290	0.59375	−0.531	0.124
0.6266	0.62500	−0.527	0.124
0.6246	0.65625	−0.520	0.128
0.6220	0.68750	−0.512	0.127
0.6199	0.71875	−0.500	0.132
0.6174	0.75000	−0.496	0.134
0.6154	0.78125	−0.485	0.134
0.6131	0.81250	−0.475	0.147
0.6106	0.84375	−0.476	0.139
0.6085	0.87500	−0.456	0.144
0.6061	0.90625	−0.457	0.146
0.6039	0.93750	−0.442	0.155
0.6016	0.96875	−0.430	0.154
0.5995	1.00000	−0.424	0.162

the chemical potential of component *B* now passes a minimum already at $x_B \approx 0.8$ and is rapidly increasing thereafter, practically indicating a "squeezing out" tendency of the *B* particles from the Type-*A* solution.

The directly calculated activity coefficients are shown in Fig. 2. Please note that the activity coefficient for component *B* in both mixtures increases with $x_B \to 0$, although the interaction strength increases. This again strongly emphasizes the importance (and sometimes perhaps dominance) of the effect of the volume changes [10].

In Fig. 2 the activity coefficients γ_α of components *A* and *B* directly obtained from the potential distribution theorem are given by full symbols. In addition we also show the activity coefficients of component *A* as obtained by integrating the Gibbs-Duhem relation using the activity coefficients of the counter component *B*. The data shown in Fig. 2 demonstrates that the activity coefficients are satisfacto-

Table 2. Excess chemical potentials $\mu_{ex,\alpha}$ and activities a_α obtained for the Lennard-Jones mixtures with $\sigma_{AA} = \sigma_{BB}$, and $\varepsilon_{AA} = 2.0 \times \varepsilon_{BB}$, simulated at $T^* = 2.0$ and $P^* = 1.755$. The shown densities values are according to $\rho^* = N\sigma_{BB}^3/V$. The data were obtained from the potential distribution theorem [2, 3].

ρ^*	x_B	$\beta\mu_{A,ex}$	$\beta\mu_{B,ex}$
0.7897	0.00000	−2.493	0.605
0.7850	0.03125	−2.488	0.582
0.7802	0.06250	−2.456	0.544
0.7754	0.09375	−2.414	0.534
0.7702	0.12500	−2.444	0.454
0.7652	0.15625	−2.418	0.428
0.7599	0.18750	−2.379	0.403
0.7548	0.21875	−2.363	0.410
0.7492	0.25000	−2.351	0.362
0.7434	0.28125	−2.342	0.326
0.7379	0.31250	−2.320	0.311
0.7320	0.34375	−2.303	0.280
0.7263	0.37500	−2.273	0.256
0.7202	0.40625	−2.236	0.234
0.7140	0.43750	−2.232	0.220
0.7081	0.46875	−2.175	0.213
0.7018	0.50000	−2.151	0.187
0.6954	0.53125	−2.122	0.168
0.6894	0.56250	−2.090	0.165
0.6828	0.59375	−2.039	0.161
0.6765	0.62500	−2.016	0.144
0.6702	0.65625	−1.967	0.142
0.6636	0.68750	−1.932	0.136
0.6571	0.71875	−1.883	0.127
0.6507	0.75000	−1.839	0.127
0.6440	0.78125	−1.802	0.120
0.6377	0.81250	−1.757	0.126
0.6311	0.84375	−1.711	0.131
0.6245	0.87500	−1.670	0.125
0.6181	0.90625	−1.610	0.130
0.6119	0.93750	−1.560	0.141
0.6054	0.96875	−1.510	0.151
0.5995	1.00000	−1.459	0.162

rily recovered, particularly when taking into account the relatively large noise in the calculated excess chemical potentials shown in Fig. 1. Moreover, since our goal was just to demonstrate the applicability of the procedure to molecular simulations, we didn't try possible further improvements of the γ_A prediction, such as interpolation and/or fitting of the data. The relatively large scatter observed for the case of $\varepsilon_{AA} = 1.33 \times \varepsilon_{BB}$ at large values of x_A suggests that an increased accuracy of μ_{ex} particularly in the dilute regime of A would be desirable.

4. Conclusion

We have determined the activity coefficients of both components of binary Lennard-Jones mixtures obtained for $T^* = 2.0$ and $\rho^* = 0.6$. Reference activity coef-

ficients were obtained by direct evaluation of the excess chemical potentials of both components applying the potential distribution theorem [2]. In addition, applying a Gibbs-Duhem integration based on the activity coefficients of the counter-component "*B*" (the solvent), calculated directly via potential distribution theorem, we were also able to recover the activity coefficients of the solvent. Both methods lead to very similar results. Therefore we suggest to determine activity coefficients of mixtures including large complex molecules by alternatively calculating chemical potentials of potentially simpler counter-constituents.

Acknowledgement

References

1. P. W. Atkins, *Physical Chemistry*. Oxford University Press, Oxford, UK (1986).
2. B. Widom, J. Chem. Phys. **39** (1963) 2808–2812.
3. T. L. Beck, M. E. Paulaitis, and L. R. Pratt, *The Potential Distribution Theorem and Models of Molecular Solutions*. Cambridge University Press, Cambrigde, UK (2006).
4. L. Verlet, Phys. Rev. **159** (1967) 98–103.
5. E. Lindahl, B. Hess, and D. van der Spoel, J. Mol. Model. **7** (2001) 306–317.
6. S. Nosé, Mol. Phys. **52** (1984) 255–268.
7. W. G. Hoover, Phys. Rev. A **31** (1985) 1695–1697.
8. J. K. Johnson, J. A. Zollweg, and K. E. Gubbins, Mol. Phys. **78** (1993) 591–618.
9. G. L. Deitrick, L. E. Scriven, and H. T. Davis, J. Chem. Phys. **90** (1989) 2370–2385.
10. A. Bem-Naim, *Solvation Thermodynamics*. Plenum Press, New York (1987).